

DAMAGE REDUCTION OF EXPLOSIVELY DRIVEN SPALLATION
BY MACHINING V-NOTCH ROWS ON THE SURFACES
OF 304 STAINLESS STEEL PLATES

T. Hiroe¹⁾, K. Fujiwara¹⁾, H. Hata¹⁾,
K. Natasato²⁾, K. Mizokami²⁾

¹⁾ **Department of Mechanical System Engineering, Kumamoto University**

Kumamoto, 860-8555, Japan
e-mail: hiroe@gpo.kumamoto-u.ac.jp

²⁾ **Graduate School of Science and technology, Kumamoto University**

Japan

Plane detonation waves generated in the explosive PETN with use of wire-row explosion technique for initiation have been applied to study on spall behaviour for circular plates of 304 stainless steel, and the slanting surface effects on the damage phenomena for conic frustums and circular cones. In this paper, V-notch rows are produced on the free surface of the square plate specimens of the same material and plane shock waves are similarly transferred from the other surface. The cross-sectional observation of tested and recovered specimens shows that remarkable effects on the reduction of spall damages have been achieved in case of appropriate V-notch configurations. The effect seems to come obviously from weakened interaction of release waves due to the dispersion of directions for reflection waves, and a hydro-code. Autodyn 2D/3D has successfully reproduced the experimental results numerically, suggesting a notch parameter chart for spall damage evaluation.

1. INTRODUCTION

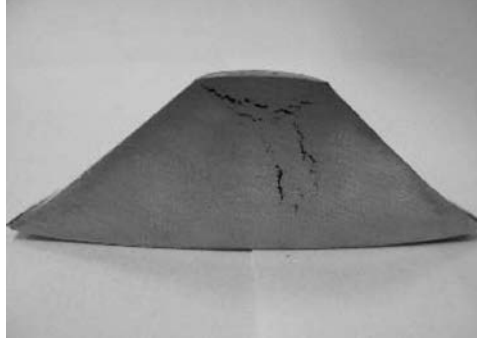
Spallation driven by direct explosive loadings [1] occurs due to tensile stresses generated by the interaction of expansion waves emerged due to the reflection of strong shock waves at the free surfaces of the structural components and other strong expansion waves coming from behind the detonation waves. Previously, the authors [2] had developed explosive loading devices producing planar detonation waves in powder pentaerythritoltetranitrate (PETN) with the use of exploding copper wire rows for initiation, showing some applications to spall tests for circular plane plates of various metallic materials, where the spalling phenomena were monitored by VISAR signals. In the following study [3, 4], spallation driven by direct explosive loads was similarly investigated for additional two types of specimens: conical frustums and circular cones of aluminum alloys and a stainless steel with variations of specimen configurations and explosive

heights, and the experimental results revealed that slanting side surfaces change the spall damage phenomena showing a possibility to reduce spall failure by applying such effects. Typical related test data are shown in Fig. 1. In this paper, V-notch rows are newly produced on the free surfaces of the stainless steel plate specimens and the explosive loading tests are performed investing appropriate V-notch configurations for spall damage reduction by means of numerical simulations.

a) circular plate



b) conical frustum



c) VISAR signal

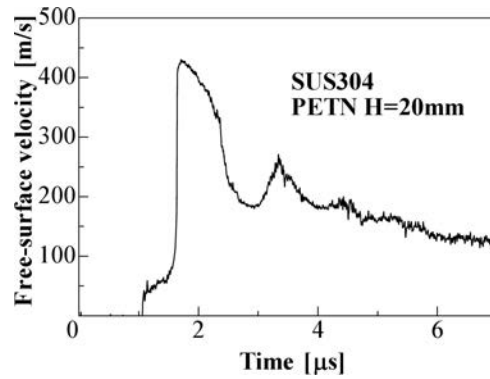


FIG. 1. Previous spall test data [2–4] of a stainless steel (SUS304) with PETN height H of 20 mm: cross-sectional photos of recovered: a) circular plate (ϕ : 50 mm, t : 20 mm), b) conical frustum (ϕ_1/ϕ_2 : 12 mm/50 mm, sloping 43.5 deg.), and c) a typical VISAR signal.

2. EXPERIMENTAL AND NUMERICAL PROCEDURE

Experiments are performed using the explosion test facilities at the Shock Wave and Condensed Matter Research Center, Kumamoto University. Schematic experimental assembly for direct-explosive impact tests is shown, with the configuration parameters of tested specimens, in Fig. 2. Slab-like installed powder PETN (0.90–0.95 g/cc) is initiated by the simultaneous explosion of parallel

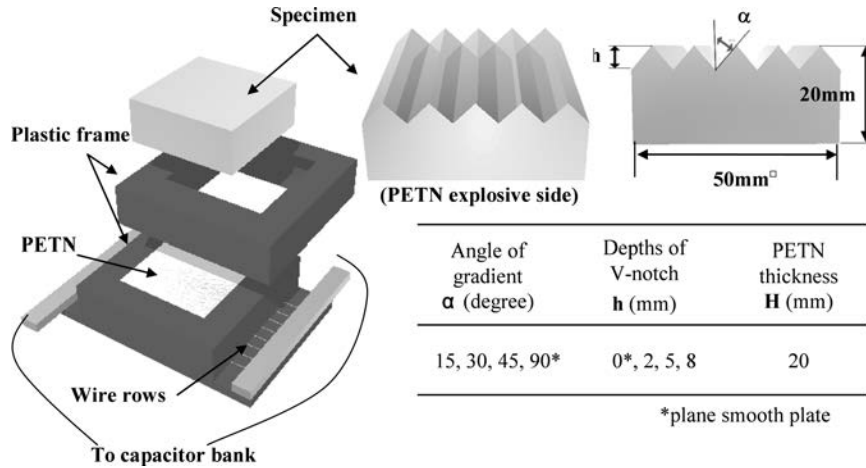


FIG. 2. Schematics of experimental assembly and the configuration parameters of tested specimens in this study.

copper wire rows (diameter: $175 \mu\text{m}$, the ratio of PETN thickness H of wire interval B , $H/B \geq 1.3$ – 1.5 for planarity [2]), placed over the entire outer surface using an impulsive discharge current from a capacitor bank of $40 \mu\text{F}$, 20kV , producing a planar detonation front in the PETN layer immediately after the initial explosion and transferring a one-dimensional triangular pressure pulse directly to the specimen plate. The PETN is installed constantly in the shape of $50 \times 50 \times 20 \text{ mm}$ and the wire intervals are 7 – 8 mm in the experiments. The specimens of 18Cr-8Ni stainless steel, JIS SUS304 are machined to the smooth quadratic plates of $50 \times 50 \times 20 \text{ mm}$ from the rolled plate of thickness of 25 mm as a basic specimen and in this study, V-notch rows were newly produced parallel to the side lines by electro-discharge machining on the free surfaces of the specimens with notch variation of height or depth h of $2, 5, 8 \text{ mm}$ and gradient angles α of $15, 30, 45$ degrees respectively. Numerical simulations are performed for all the experiments and additional conditions using a hydro-code: Autodyn 2D/3D based on the finite difference method, and Euler coordinates, material data or 304 stainless steel [5], PETN and plastics built in the code, and two-dimensional analysis with mesh division of $0.2 \times 0.2 \text{ mm}$, are basically employed here. Stress criterion of SUS304: $\sigma_{sp} = 3.5 \text{ GPa}$ previously obtained [2] shown in Fig. 1c for spall damage has been also adopted.

3. EXPERIMENTAL RESULTS

In all the explosion tests, experimental assembly shown in Fig. 2 was installed inside a cushion-filled chamber set in the pit and the tested specimens were successfully recovered without secondary damage. The recovered speci-

mens were separated halves by a fine-cutter machine perpendicularly to V-notch rows and the emerged cross-sectional surfaces were lapped. Spall damages of the specimens were observed in the cross-sections for all the cases. Figure 3 shows cross-sectional photos of tested specimens for all the notched specimens, and macroscopic observation indicates three types of damage phenomena in the cross-sections. In the first type, spall damages extended parallel to the plate surfaces or perpendicular to stress wave propagation. It is the ordinary spallation caused by the interaction of the expansion wave reflected at the free surfaces of the plate specimen and other expansion wave coming from behind the detonation. Here it is called “horizontal spall”, as shown in the figure. In the second type called “vertical spall”, spall damages extended along the central line of each ridge of the V-notch rows. This type of damages are obviously caused by the interaction of expansion waves reflected at a pair of slanting surfaces on every V-notch row, and then in this case, ordinary spallation does not appear because of reduction of the reflected expansion waves. Finally, in the third type called “no spall”, only the case of $\alpha = 15^\circ$, $h = 8$ mm, spall damage is remarkably reduced almost to zero under the macroscopic observation, where around 0.4 mm cracking is critical. Additionally, a mixed type of horizontal and vertical spall exists consequently what is seen in the case of $\alpha = 30^\circ$, $h = 5$ mm.

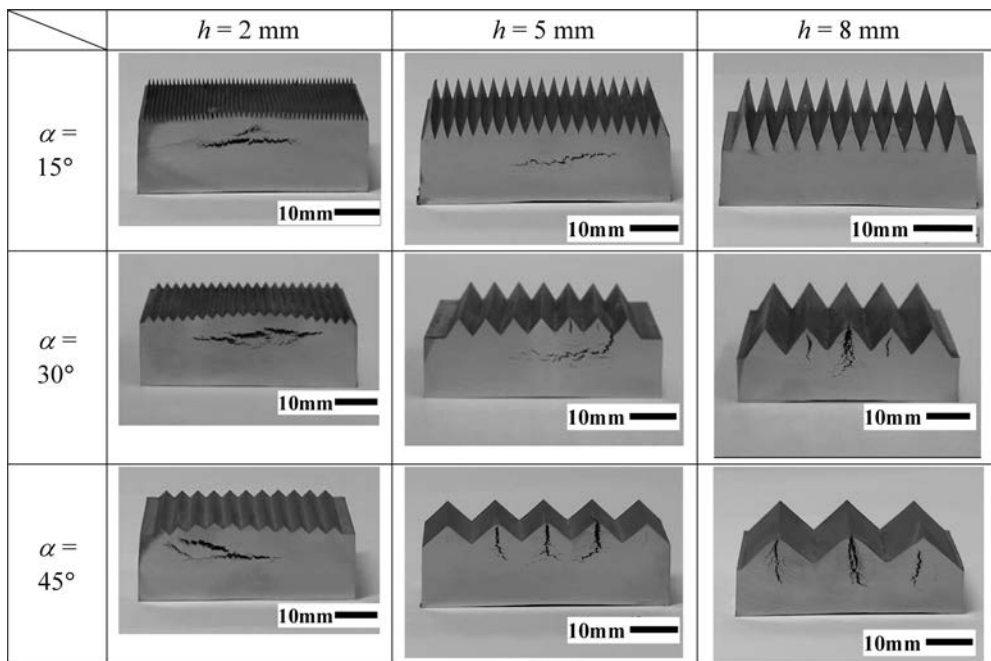


FIG. 3. Cross-sectional photos of tested, recovered and half-cut specimens for all the notched specimens.

4. NUMERICAL RESULTS

In preliminary investigation, numerical overall spall damage phenomena in the cross-sections generated 3D analysis of Autodyn do not make essential difference from those by 2D analysis, and actually in this study, 2D numerical simulation successfully reproduced experimental cross-sectional spall damages for all the cases. Figure 4 shows typical three types of numerical damage distributions in the cross-sections based on stress criterion, where lowermost density elements are represented as voids. They correspond practically well to experimental results shown in Fig. 3 including no spall type, where separation of two meshes is defined as numerical minimum damage coinciding with experimental macroscopic observation. Next in order to verify the emerged damage phenomena on the stress criterion base, stresses in the specimens were examined for all the test cases. Figure 5 shows typical numerical time-histories of spatial distributions




Types	Horizontal spall	Vertical spall	No spall damage
Typical examples			
Parameter	$\alpha = 30^\circ, h = 2 \text{ mm}$	$\alpha = 45^\circ, h = 8 \text{ mm}$	$\alpha = 15^\circ, h = 8 \text{ mm}$

FIG. 4. Typical three types of numerical simulation results for the cross-sections of explosively loaded, notched specimens with use of Autodyn 2D. Solid lines show 10 mm.

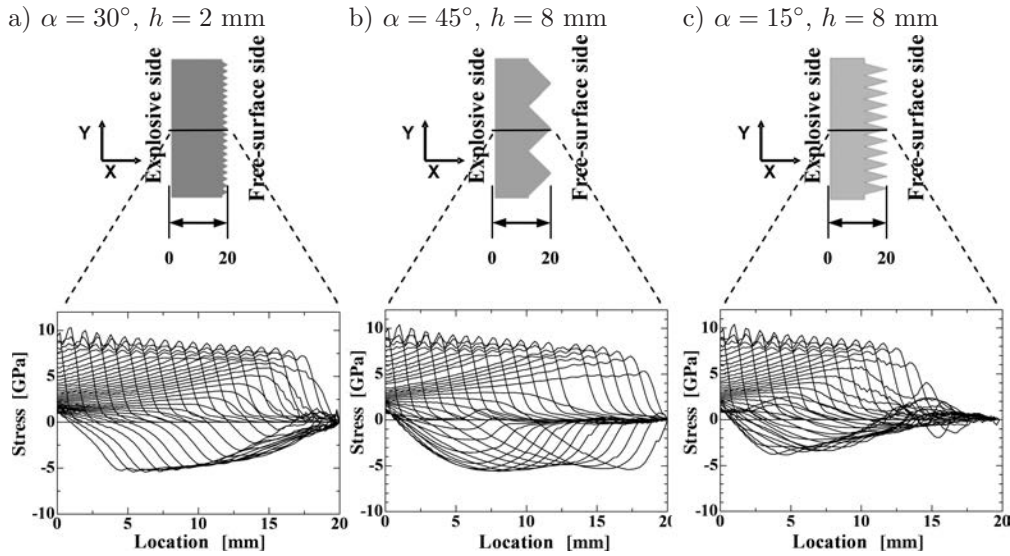


FIG. 5. Typical numerical time-histories of spatial distributions of stress $\sigma_x (\cong \sigma_y)$ in the specimens shown in Fig. 4.

butions of stress $\sigma_x (\cong \sigma_y)$, along the central line from the bottom of the plate to the peak of the V-notch ridge in the same specimens in Fig. 4, where x and y are the directions of thickness and width of the plate perpendicular to the notch rows, and plus stress denotes a compressive one, and failure criterion is not used here. It is seen that in cases (a) and (b), reflected tensile stresses soon go much over the stress criterion value σ_{sp} of 3.5 GPa, and in case (c) the stresses barely reach the value in a short period after some time period from the reflection at the restricted narrow area. The damages in the specimens with lowest notch height of 2 mm in the case (a) resemble that of plane smooth plate without slant surface effect, and it follows from small stress growth and interaction after reflection. Such stress distributions explain well all the spall phenomena in this study.

5. DISCUSSION

Experimental and numerical results suggest that there exists a notch parameter chart for spall damage evaluation. In the numerical simulation for building the chart, 2D analysis for the model including only one ridge of V-notch assuming wide plate with large number of notch rows, was adopted for simplicity as the damage evaluation model of central part in the specimen, which is confirmed appropriately as a practical use by preliminary examination. Figure 6 represents a spall damage evaluation chart derived from the experimental results and numerical simulation, where simplified 2D models were analysed changing the parameters of notch height h and a half wavelength of notch rows y with the intervals of 1 mm and 0.2 mm respectively. The area where the values of y are under numerical critical points for every notch height h represents the notch configuration, where spall failure does not occur. The effect of such slant sur-

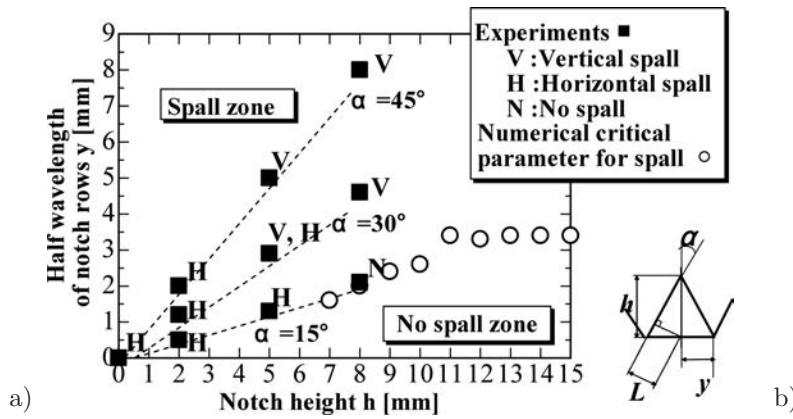


FIG. 6. a) A spall damage evaluation chart of explosively loaded V-notched plates with the height of 20 mm for explosives and plates based on the results of this study, and b) – the related configuration parameters of V-notch.

faces comes obviously from weakened interaction of released waves due to the dispersion of directions for reflection waves, but in the area where y is above numerical critical value, the spall failure is inevitable. Especially in the area where y is over the value of 3.4 in the figure, vertical or inner notch ridge spall occurs because release waves reflected at the slant surfaces grow enough to spallation. Distance L in (b) is also related with the inner notch ridge failure. On the contrary, in the spall failure area where y is under the value and furthermore notch height h is small, interaction effect of slant surfaces of V-notch rows is diminished and horizontal or ordinary spall occurs.

6. CONCLUSION

Reduction of spall failure for plates loaded directly by plane detonation wave generator was investigated machining V-notch rows at the free surfaces. Experimental and numerical results revealed remarkable effect of the slant surfaces V-notches, and a notch parameter chart for spall damage evaluation was suggested successfully. The damage reduction method introduced in this study can be applied to explosively loaded plates with other dimensions, in cooperation with numerical simulation. In the future study, more simplified system will be required for the practical use.

REFERENCES

1. F. TULER and B. M. BUTCHER, *Criterion for the Time Dependence of Dynamic Fracture*, International Journal of Fracture Mechanics, **4**, 431–437, 1968.
2. T. HIROE, K. FUJIWARA, MATSUO HIDEO, and N. N. THADHANI, *Explosively Produced Spalling in Metals and Its Loading Effects*, Proceedings of the 4th International Symposium on Impact Engineering, A. CHIBA, S. TANIMURA, and K. HOKAMOTO [Eds.], Elsevier Science Ltd., Oxford, 851–856, 2001.
3. T. HIROE, K. FUJIWARA, H. HATA, and Y. D. TSUTSUMI, *Spall Fracture of Metallic Circular Plates, Vessel Endplates and Conical Frustums Driven by Direct Explosive Loads*, Proceedings of the Conference of the APS Topical Group on Shock Compression of Condensed Matter, M. ELERT, M. D. FURNISH, R. CHAU, N. HOLMES and J. NGUYEN [Eds.], American Institute of Physics, New York, 537–540, 2007.
4. K. NAKASATO, T. HIROE, K. FUJIWARA, H. HATA, *The Effect of Slanting Side Surfaces on the Spall Fracture Behaviour of Metallic Plates Induced by Explosive Shock Waves and Its Application to Novel Plates Structures for Damage Reduction*, Proceedings of International Workshop on Explosion, Shock Wave and Hypervelocity Phenomena 2008, pp. 54–57, Kumamoto University, Kumamoto, 2008.
5. D. J. STEINBERG, *Equation of State and Strength Properties of Selected Materials*, LLNL Report UCRL-MA-106439, 1991.

Received December 16, 2010.
